The paper was published in the proceedings of the 7th International Conference on Earthquake Geotechnical Engineering and was edited by Francesco Silvestri, Nicola Moraci and Susanna Antonielli. The conference was held in Rome, Italy, 17 – 20 June 2019.

Earthquake Geotechnical Engineering for Protection and Development of Environment and Constructions – Silvestri & Moraci (Eds)
© 2019 Associazione Geotecnica Italiana, Rome, Italy, ISBN 978-0-367-14328-2

Behavior of a Gulf of Mexico clay under variable-strain cyclic loads

V. Taukoor & S.M. Olson
University of Illinois at Urbana-Champaign, Urbana-Champaign, USA

C.J. Rutherford
Iowa State University, Iowa, USA

ABSTRACT: To better understand the influence of variable-strain time histories on the cyclic and post-cyclic behavior of offshore soft clays, nine undrained triaxial tests were performed on a Gulf of Mexico clay. The specimens were subjected to strain-controlled cyclic loading, immediately followed by undrained monotonic compression loading. The specimens were consolidated to overconsolidation ratios of 1, 2, and 3. Three combinations of cyclic strain amplitudes were investigated, namely "ramp up" (cyclic axial strain ε_c = 0.5→1→1.5→2.0→2.5→3%), "ramp down" (ε_c = 3→2.5→2.0→1.5→1→ 0.5%) and "ramp up and down" (ε_c = 0.5→1.5→3→1.5→0.5%). The results illustrate that both the sequence of cyclic loads and specimen OCR affected the normalized cyclic shearing resistance and shear modulus degradation, but had a lesser effect on the cyclic load-induced normalized excess pore pressure. All the tests followed a dilative stress path during post-cyclic monotonic loading and reached the same Mohr-Coulomb failure envelope defined from monotonic undrained triaxial tests.

1 INTRODUCTION

When soft clays are subjected to repeated undrained loads, they experience a gradual generation of excess porewater pressure (PWP) and a progressive de-structuration of the clay structure. The net result is a progressive loss in their shearing resistance and shear stiffness. The magnitude and the rate of this cyclic degradation are functions of the loading conditions (e.g., Dobry and Vucetic 1987; Mortezaie and Vucetic 2013; Wichtmann et al. 2013), including frequency and cyclic stress ratio for stress-controlled tests (or cyclic shear strain, γ_c, for strain-controlled tests), as well as soil stress state (e.g., Le at al. 2014), including maximum past pressure ($\sigma'_{v,max}$) or preconsolidation pressure (σ'_p), initial effective stress (σ'_{vo}), and coefficient of earth pressure (k_0). Cyclic degradation poses a significant hazard to infrastructure founded on offshore soft clays such as oil platforms, towers, pipelines, cables, and subsea or floating systems, and can be caused by "non-standard" events involving variations with time of cyclic displacements and loads. Examples of non-standard events are earthquake loads (e.g., Soroush et al. 1996) and storm waves, currents and gusts (e.g., Andersen and Høeg 1991). This paper investigates the effect of variable-strain time histories on the cyclic degradation and post-cyclic shear strength of a Gulf of Mexico (GOM) clay. The testing equipment used for this study is a servo-pneumatic system designed to perform both monotonic and cyclic triaxial tests.

2 GULF OF MEXICO CLAY

The GOM clay used was sampled during a May 2012 commercial cruise with a Jumbo Piston Core (JPC) sampler from about 3000 m below sea level in the Walker Ridge area of the Gulf of Mexico basin. Details about the JPC sampling technique can be found in Silva and Bryant (2000).

Table 1. Summary of the testing program

Test	w_o (%)	$\sigma'_{cons,1}$ [a] (kPa)	$\sigma'_{cons,2}$ [b] (kPa)	Pre-cyclic OCR	Cyclic axial single strain amplitude history (%)	Type of cyclic test
VS-CTX1	104	194	194	1.0	0.5→1.0→1.5→2.0→2.5→3	Ramp up
VS-CTX2	111	185	185	1.0	3.0→2.5→2.0→1.5→1.0→0.5	Ramp down
VS-CTX3	114	206	206	1.0	0.5→1.5→3.0→3.0→1.5→0.5	Ramp up and down
VS-CTX4	116	247	122	2.0	0.5→1.0→1.5→2.0→2.5→3	Ramp up
VS-CTX5	119	259	128	2.0	3.0→2.5→2.0→1.5→1.0→0.5	Ramp down
VS-CTX6	117	221	110	2.0	0.5→1.5→3.0→3.0→1.5→0.5	Ramp up and down
VS-CTX7	119	255	87	2.9	0.5→1.0→1.5→2.0→2.5→3	Ramp up
VS-CTX8	118	242	87	2.8	3.0→2.5→2.0→1.5→1.0→0.5	Ramp down
VS-CTX9	116	233	77	3.0	0.5→1.5→3.0→3.0→1.5→0.5	Ramp up and down

The soft, greenish-grey GOM clay used for the tests was retrieved from a depth of 7.9 m to 8.4 m below the seabed. It had the following properties: in-situ water content, w_0 = 104 – 116%; total unit weight, γ_T = 14 – 15 kN/m^3; liquid limit, w_L = 95%; plastic limit, w_P = 41%; plasticity index, I_p = 54%; clay fraction, CF = 77%; specific gravity, G_s = 2.77; in-situ effective vertical stress, σ'_{vo} = 30 – 33 kPa; preconsolidation pressure, σ'_p = 55 – 58 kPa. Except for very thin horizontal to sub-horizontal silt seams, the GOM clay was homogeneous with no foraminifera, shells, air pockets or organics.

3 TESTING PROGRAM

A summary of the testing program is shown in Table 1. The specimens, trimmed to an average diameter of 37.6 mm and an average height of 74.5 mm (average H/D = 2.0), were normally consolidated to a maximum value of equal all-around stress $\sigma'_{v,max}$ corresponding to 185 – 259 kPa. To induce overconsolidation, cell pressure was subsequently decreased to the desired consolidation stress. Specimens were allowed to reach EOP rebound at the desired consolidation stress prior to cyclic shearing. The induced OCRs were 1, 2 and 3. Following consolidation to the desired OCR, the drainage valves were shut off and the specimens were subjected to 6 consecutive packets of 200 sinusoidal cyclic axial strain cycles (ε_c ranging between 0.5% and 3%) at a frequency of 0.5Hz. It is noted that in undrained conditions, the cyclic shear strain γ_c is 1.5 times ε_c. The specimens in tests VS-CTX1, VS-CTX4 and VS-CTX7 were subjected to a "ramp up" type cyclic strain history, from 0.5% to 3% in increments of 0.5%. Tests VS-CTX2, VS-CTX5 and VS-CTX8 had a "ramp down" type of cyclic strain history, from 3% to 0.5% in decrements of 0.5% for each packet of cycling. VS-CTX3, VS-CTX6 and VS-CTX9 involved a "ramp up and down" style of cyclic strain history, with ε_c = 0.5%, 1.5%, 3%, 3%, 1.5%, and 0.5%. Following the final cyclic packet, the cyclic shear-induced excess PWP was allowed to equalize and the specimens were subjected to monotonic undrained compression.

4 RESULTS AND DISCUSSION

Figure 1 through Figure 3 show the results of VS-CTX1 through VS-CTX3, respectively, in terms of:

1. [$\Delta\sigma_{cyc}(TC)/\sigma'_{v,max}$] vs. number of cycles (N), where $\Delta\sigma_{cyc}(TC)$ is the cyclic deviatoric shearing resistance in triaxial compression.
2. G/G_1 vs. N, where G is the undrained shear modulus in any given cycle and G_1 is the undrained shear modulus measured in the first cycle of loading of the first packet. Shear

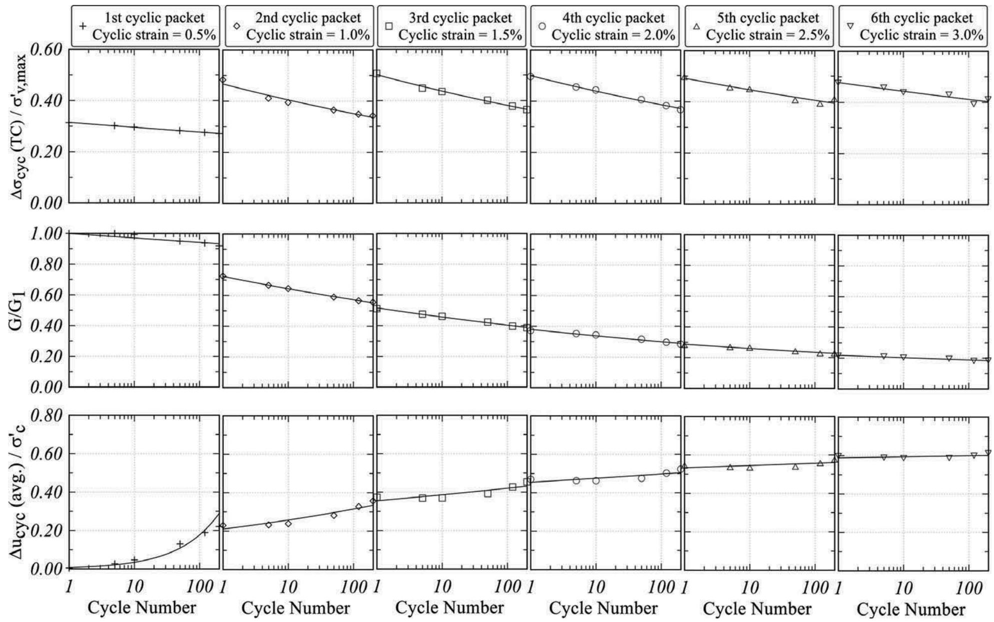

Figure 1. Results of the cyclic portions of test VS-CTX1

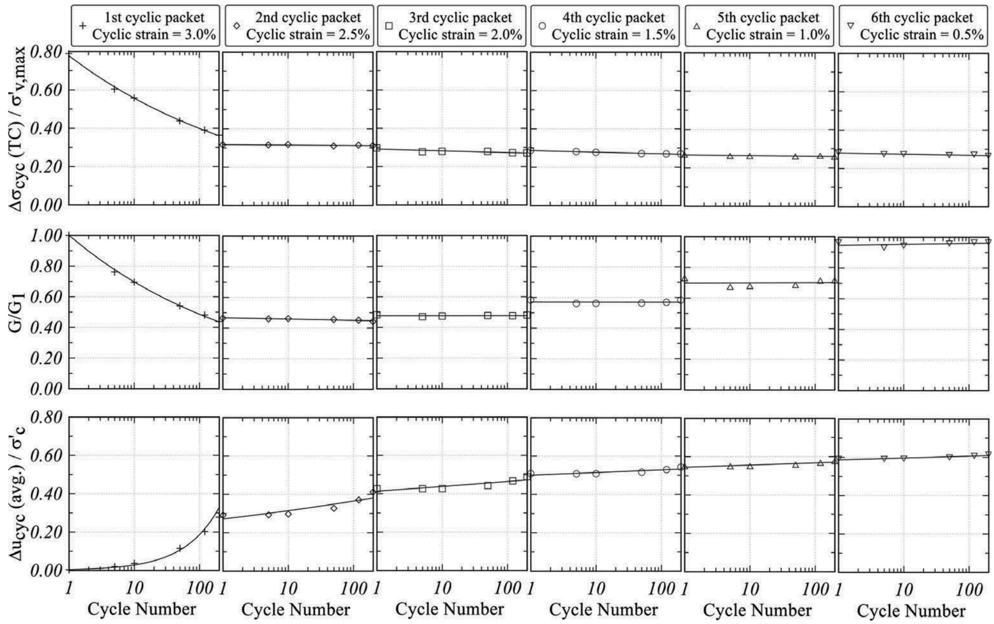

Figure 2. Results of the cyclic portions of test VS-CTX2

modulus G was calculated as the slope of a line connecting the apexes of the shear stress-shear strain loops.

3. [Δu_{cyc}(avg)/σ'_c] vs. N, where Δu_{cyc}(avg) is the cyclic shear-induced excess porewater pressure (average of compression and extension phases of a cycle) and σ'_c is the effective stress of the specimen prior to cycling.

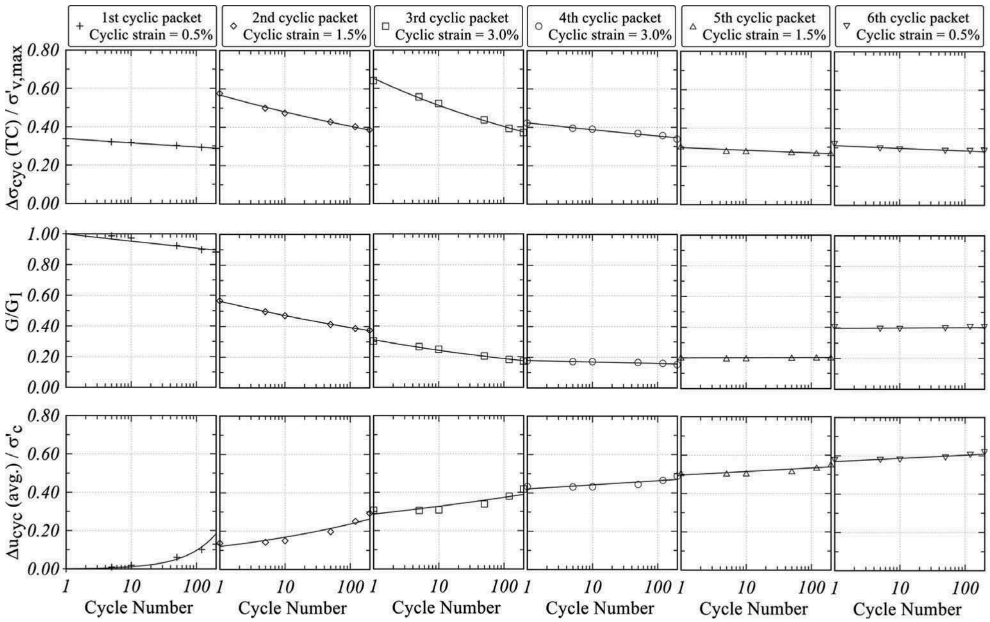

Figure 3. Results of the cyclic portions of test VS-CTX3

4.1 *Normalized cyclic shear resistance*

The normalized shearing resistance, equivalent to half of $\Delta\sigma_{cyc}(TC)/\sigma'_{v,max}$, is influenced by the cyclic strain history provided the cyclic axial strain amplitude is smaller than about 2 – 3%, herein referred to as "$\varepsilon_{c,lim}$" (more detail is provided later). The shearing resistance increases with increasing cyclic strain for the "ramp up" tests (VS-CTX1, VS-CTX4 and VS-CTX7) up to about $\varepsilon_c \sim 2 – 3\%$ (packet 3 or 4), after which the shearing resistance stays fairly constant. For the "ramp up and down" tests (VS-CTX3, VS-CTX6 and VS-CTX9), the shearing resistance increases with increasing cyclic strain; however, once $\varepsilon_c \sim 2 – 3\%$ is applied, a subsequent decrease in cyclic strain amplitude does not cause a significant change in shearing resistance. In the "ramp down" tests (VS-CTX2, VS-CTX5 and VS-CTX8), once $\varepsilon_c \sim 2 – 3\%$ is applied in packet 1, the subsequent decrease in cyclic strain (packets 2 – 5) does not cause the shearing resistance to decrease significantly. Based on the above, $\varepsilon_{c,lim}$ is defined as the cyclic axial strain that once applied, damages the soil structure to an extent such that further cyclic straining does not cause a significant change in shearing resistance.

Within a given packet at a given strain level ($< \varepsilon_{c,lim}$) and given pre-cyclic OCR, the rate of degradation in shearing resistance is fairly constant (the frequency of cycling was kept constant at 0.5 Hz). However, with increasing pre-cyclic OCR, the rate of degradation in shearing resistance decreases. This is possibly due to the fact that overconsolidated clays (OC clays) have a tendency to dilate when sheared and to generate negative excess porewater pressures. Thus, the loss in shearing resistance for OC clays is smaller. This is also in line with the observations that OC clays experience a slower degradation of their fabric, as shown by their relatively smaller values of degradation parameter "t" (Dobry and Vucetic 1987).

a. Effective equal all-around pressure during first stage of consolidation
b. Effective equal all-around pressure prior to cycling

4.2 *Normalized undrained shear modulus*

One way to quantify cyclic shear modulus degradation within a packet is through degradation parameter "t", whereby $G/G_1 = N^{-t}$ (e.g., Idriss et al. 1978); the larger the degradation

Table 2. Degradation parameter "t" computed for individual packets of cycling

Test	Type of cyclic test	Packet #1	Packet #2	Packet #3	Packet #4	Packet #5	Packet #6
VS-CTX1	Ramp up	0.013	0.051	0.053	0.052	0.044	0.033
VS-CTX2	Ramp down	0.157	0.008	0.000	0.000	0.000	0.000
VS-CTX3	Ramp up and down	0.021	0.079	0.110	0.026	0.000	0.000
VS-CTX4	Ramp up	0.036	0.041	0.050	0.054	0.059	0.057
VS-CTX5	Ramp down	0.135	0.000	-0.008	-0.009	-0.009	-0.003
VS-CTX6	Ramp up and down	0.029	0.064	0.100	0.025	-0.009	-0.022
VS-CTX7	Ramp up	0.105	0.065	0.043	0.039	0.039	0.030
VS-CTX8	Ramp down	0.118	0.006	-0.006	-0.011	-0.022	-0.014
VS-CTX9	Ramp up and down	0.022	0.059	0.099	0.021	-0.015	-0.027

parameter "t", the more damage the clay fabric has suffered. The degradation parameters during the individual packets of cycling for the nine tests are summarized in Table 2. For the "ramp up" tests (VS-CTX1, VS-CTX4 and VS-CTX7), the degradation parameter "t" generally increases with applied cyclic strain. However, once $\varepsilon_c > \varepsilon_{c,lim}$ is applied, "t" tends to a given value (which decreases with increasing pre-cyclic OCR). Possible reasons for this are that at strain levels above $\gamma_{c,lim}$, the values of G are comparable to one another and the fabric of the clay is so damaged such that the change in G/G_1 with cycling becomes negligible. Thus, the potential for further G/G_1 degradation is small.

For the "ramp down" tests (VS-CTX2, VS-CTX5 and VS-CTX8), there was a significant decrease in G/G_1 in the first packet. Subsequently reducing the cyclic strain amplitude mobilized larger values of G/G_1 and values of "t" that are close to zero or sometimes negative (see Table 2). These can be explained by the fact that reducing the imposed cyclic strain causes a "ride up" the G/G_{max} - γ curve (e.g., Vucetic and Dobry 1991), mobilizing a larger value of G. In the authors' opinion, a true "regain in stiffness" under the circumstances described is unlikely for 2 reasons: 1) there is no increase in effective stress 2) the fabric of the clay is already damaged and cannot sustain any stiffness increase without reconsolidation to a larger $\sigma'_{v,max}$. The "ramp up and down" tests (VS-CTX3, VS-CTX6 and VS-CTX9) also showed degradation of G/G_1 within packets and from packet to packet for cyclic axial strains up to $\varepsilon_{c,lim}$. Beyond $\varepsilon_{c,lim}$, the G/G_1 degradation within packets became negligible (in some instances, increased; see negative values of "t") and there was a noticeable jump in G/G_1 from packet to packet. The same explanation given for the "ramp down" tests (i.e., smaller cyclic strains mobilize larger values of G) can be used to explain the values of "t" for the "ramp up and down" tests.

4.3 *Cyclic shear-induced excess porewater pressure build-up*

In general, the higher the pre-cyclic OCR, the smaller the $[\Delta u_{cyc}(avg)/\sigma'_c]$, as shown in Table 3. In all the tests, across pre-cyclic OCRs of 1 to 3 and irrespective of the type of test, the first packet of cycles showed the largest and fastest generation of excess PWP. The

Table 3. Some results from the cyclic and monotonic portions of the tests

Test	Type of cyclic test	$\Sigma[\Delta u_{cyclic}]/\sigma'_{v,max}$ [a]	σ'_{PC} [b] (kPa)	OCR_{PC} [c]	$[\Delta u_{monotonic}/\sigma'_{v,max}]$ [d]	$\Delta u_{total}/\sigma'_{v,max}$ [e]	$s_{u,PC}$ (TC)$/\sigma'_{PC}$ [f]
VS-CTX1	Ramp up	0.52	50	3.9	0.055	0.58	0.90
VS-CTX2	Ramp down	0.54	58	3.2	0.080	0.62	0.73
VS-CTX3	Ramp up and down	0.54	60	3.4	0.091	0.63	0.82
VS-CTX4	Ramp up	0.07	55	4.5	0.021	0.09	0.79
VS-CTX5	Ramp down	0.17	57	4.5	0.039	0.21	0.90
VS-CTX6	Ramp up and down	0.15	47	4.7	0.030	0.18	0.81
VS-CTX7	Ramp up	0.05	47	5.4	0.030	0.08	0.74
VS-CTX8	Ramp down	0.09	44	5.5	0.041	0.13	0.87
VS-CTX9	Ramp up and down	0.06	48	4.9	0.043	0.11	0.73

generation of [Δu_{cyc}(avg)/σ'_c] in subsequent packets decreased such that in packet 6, regardless of whether the test was a "ramp up", a "ramp down" or a "ramp up and down" type, the cyclic shear-induced excess porewater pressure reaches a nearly constant value. Thus [Δu_{cyc} (avg)/σ'_c] is not affected by strain history. A possible explanation for this is that PWP generation is highly sensitive to fabric damage, more so than G/G_1 or cyclic shear resistance. Once a clay specimen has been cycled through (ε_c = 0.5 – 3%) and the fabric is damaged, less subsequent fabric damage can occur and further excess PWP is small.

4.4 *Post-cyclic undrained compression*

Following the cyclic part of the test, with the drainage valves still closed, the PWP generated within the specimen was allowed to equalize, following which a strain-controlled undrained monotonic compression test was run. The strains at failure, defined as the strains at the maximum shear stress, were between 4% and 8%, and did not seem to be influenced by prior cyclic strain history. The effective stress after PWP equalization, termed post-cyclic effective stress or σ'_{PC}, and the post-cyclic OCR (i.e., $OCR_{PC} = \sigma'_{v,max}/\sigma'_{PC}$), are shown in Table 3. The strain rate used was 0.55%/hour on average (0.36 – 0.71 %/hr). Figure 4 shows the plot of the post-cyclic undrained shear strength normalized by σ'_{PC} against OCR_{PC}. Also shown on the plot are the results of undrained monotonic triaxial compression tests run on GOM clay without pre-cycling (in a SHANSEP-type space, Ladd and Foott 1974). The results from the varying strain series of tests follow the same trend as the monotonic tests without pre-cycling. Thus, the final state of a specimen as defined by its OCR_{PC} seems to influence the undrained shear strength at failure, rather than prior cyclic strain history or pre-cyclic OCR. Figure 5 shows the stress paths for all post-cyclic monotonic compression tests from the nine varying strain tests, VS-CTX CU1 through VS-CTX CU9 (note: CU implies monotonic undrained triaxial compression). Included are the drained fully-softened failure envelope obtained from a series of tests run on GOM clay of similar mineralogical composition and some drained fully-softened failure envelopes suggested in the literature (Murali 2011; Silva et al. 2000; Mesri and

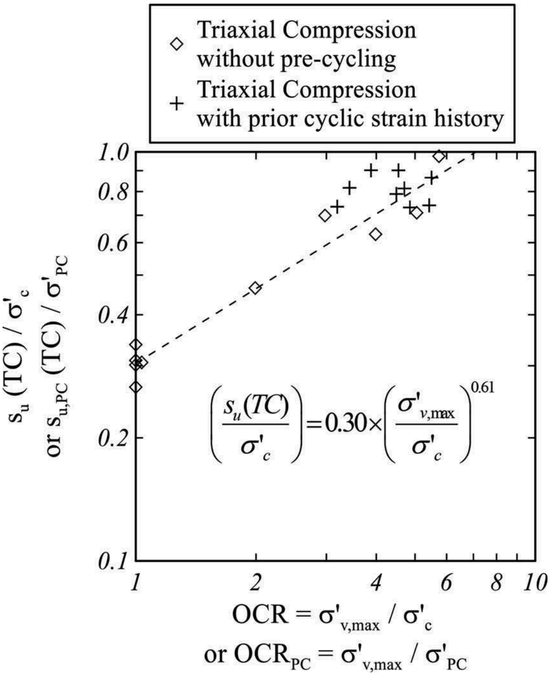

Figure 4. Showing the normalized undrained shear strength vs. post-cyclic OCR

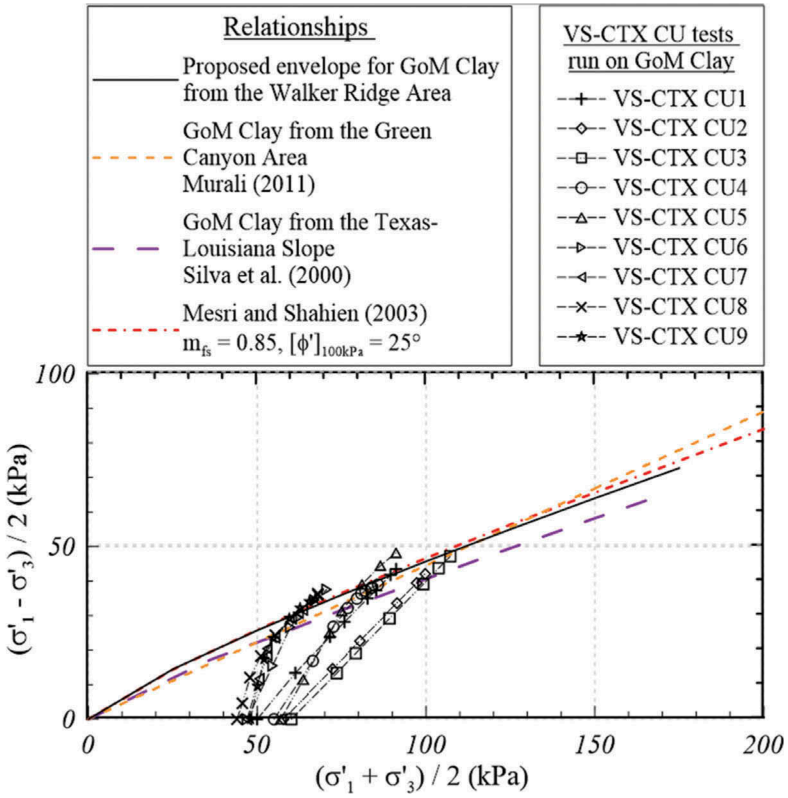

Figure 5. Showing the monotonic undrained triaxial compression portions of VS-CTX1 – VS-CTX9 plotted in a stress-path space. Included are some failure envelopes reported in the literature.

Shahien 2003). All the nine tests showed a dilative behavior but end on the same failure envelope. The failure envelope represents large strain behavior, which is controlled by mineralogy and not influenced by factors such as the original fabric and aging. Hence, the same failure envelope is applicable for the GOM clay brought to failure monotonically or through a combination of cyclic and monotonic straining.

a. Sum of the cyclic shear-induced excess porewater pressure normalized by $\sigma'_{v,max}$
b. Post-cyclic effective stress (effective stress at the end of cycling), after porewater pressure equalization throughout the specimens
c. Ratio of the maximum past effective stress to the post-cyclic effective stress ($\sigma'_{v,max}/\sigma'_{PC}$)
d. Excess porewater pressure generated at failure (defined at maximum shear stress) during post-cyclic monotonic compression
e. Total normalized PWP generated during the cyclic and post-cyclic tests, i.e., sum of $\Sigma[\Delta u_{cyclic}]/\sigma'_{v,max}$ and $[\Delta u_{monotonic}/\sigma'_{v,max}]$
f. Ratio of the post-cyclic undrained shear strength (triaxial compression mode) to the post-cyclic effective stress, σ'_{PC}

5 CONCLUSIONS

Based on a series of strain-controlled cyclic triaxial tests with variable cyclic strain history on a GOM clay, the following conclusions can be drawn.

1. The cyclic shearing resistance and shear modulus of GOM clay are significantly influenced by the magnitude of applied cyclic strain and the cyclic strain history. The strains at failure observed in the post-cyclic undrained monotonic triaxial compression tests and the net excess PWP (cyclic and monotonic) do not seem to be affected by prior cyclic strain history.
2. If the applied cyclic axial strain is larger than 2 – 3% (termed "$\varepsilon_{c,lim}$"), the clay fabric gets damaged such that further straining does not cause significant changes in shear resistance, shear modulus degradation and cyclic shear-induced excess PWP.
3. The cyclic shear modulus degradation of GOM clay, assessed through the use of degradation parameter "t", is heavily influenced by the magnitude of applied cyclic strain and pre-cyclic OCR. However, if the applied cyclic strain is larger than $\varepsilon_{c,lim}$, further cyclic shear modulus degradation is relatively small ("t" tends to zero).
4. For a pre-cycled specimen, cyclic shear modulus in tests involving decreasing cyclic strain amplitude can increase. One explanation is that smaller cyclic strains mobilize larger values of G (analogy was given to a typical G/G_{max} - γ_c curve).
5. The post-cyclic undrained shear strength normalized by the post-cyclic effective stress is a function of the post-cyclic OCR. All the pre-cycled tests showed a dilative behavior but end on the same failure envelope defined in an effective stress space, irrespective of cyclic strain history.

REFERENCES

Andersen, K. H. and Høeg, K. (1991). Deformations of soils and displacements of structures subjected to combined static and cyclic loads. In Proceedings of the 10th European Conference on Soil Mechanics and Foundation Engineering, Vol 4., 1147 – 1158.

Dobry, R. and Vucetic, M. (1987). State-of-the-art report: Dynamic properties and response of soft clay deposits. Proc. of the Int. Symposium on Geotechnical Engineering of Soft Soils, Eds, M. J. Mendoza and L. Montanez, Sociedad Mexicana de Mecanica de Suelos, Mexico City, Vol. 2, 51–587.

Idriss, I. M., Dobry, R. and Singh, R. D. (1978). Non-linear behavior of soft clays during cyclic loading. Journal of the Geotechnical Engineering Division, ASCE, GT12, 1427-1447.

Ladd, C. C. and Foott, R. (1974). New Design Procedure for Stability of Soft Clays. Journal of Geotechnical Engineering, Vol. 100 (GT7), 763–786.

Le, T. M. H., Eiksund, G. R. and Strøm, P. J. (2014). Cyclic Behavior of an Overconsolidated Marine Clay at Sheringham Shoal Offshore Wind Farm. Journal of Ocean and Wind Energy, The International Society for Offshore and Polar Engineers, Vol.1 (1), 59–564.

Mesri, G. and Shahien, M. (2003). Residual Shear Strength Mobilized in First-Time Slope Failures. J.of Geotech. and Geoenv. Eng., Vol. 129 (1), 12-31. DOI: 10.1061/(ASCE)1090-0241(2003)129:1(12).

Mortezaie, A. and Vucetic, M. (2013). Effect of Frequency and Vertical Stress on Cyclic Degradation and Pore Water Pressure in Clay in the NGI Simple Shear Device. J. Geotech. Geoenviron. Eng., Vol. 139(10), 1727–11737. DOI:10.1061/(ASCE)GT.1943-5606.0000922.

Murali, M. (2011). Characterization of Gulf of Mexico clay using automated triaxial testing. Master's Thesis, Texas A&M University, College Station, Texas.

Soroush, A., Morgenstern, N.R., Robertson, P.K., and Chan, D. (1996). The earthquake deformation analysis of the Upper San Fernando Dam. Proc. of the Int. Symposium on Seismic and Environmental Aspects of Dams Design: Earth, Concrete and Tailing Dams, Santiago, Chile, Vol. 1., 405–4418.

Silva, A. J. and Bryant, W. R. (2000). Jumbo Piston Coring in deep water Gulf of Mexico for seabed geohazard and geotechnical investigations. Proceedings of the 10th International Offshore and Polar Engineering Conference, Seattle, USA, 424–4432.

Silva, A., Baxter, C., Bryant, W., Bradshaw, A. and LaRosa, P. (2000). Stress-Strain Behavior and Stress State of Gulf of Mexico Clays in Relation to Slope Processes. Proceedings of the Offshore Technology Conference, Houston, Texas. 1–10. DOI:10.4043/12091-MS

Vucetic, M. and Dobry, R. (1991). Effect of soil plasticity on cyclic response. Journal of Geotechnical Engineering, ASCE, Vol. 117 (1), 89–107. DOI: 10.1061/(ASCE)0733-9410(1991)117:1(89)

Wichtmann, T., Andersen, K. H., Sjursen, M. A. & Berre, T. (2013). Cyclic tests on high-quality undisturbed block samples of soft marine Norwegian clay. Canadian Geotechnical Journal, Vol. 50, 400–4412. DOI: 10.1139/cgj-2011-0390.